Chapter 14
DC Microgrid Control

Marian Gaiceanu, Iulian Nicusor Arama and Iulian Ghenea

Abstract The current challenges of the current power system are to face-up with the integration of the increased renewable energy sources, energy storage systems, access to the energy market in an optimal manner, reconfiguration under faults using microgrid concept, being capable to assure more flexibility, and stability, through advanced control. The chapter makes a modern introduction into the DC microgrid architectures and their control. As the most used control into the DC microgrids, the hierarchical control is presented. In order to guide the readers, the most used standards related to DC microgrids are presented. As case study, the advanced control of the utility converter has been developed and simulated in Matlab/Simulink. Nowadays, the security protection of the energy network is a concern. An introduction to cyber-physical system (CPS) related to the power system field is presented.

Keywords Microgrid · Control · Cyber-physical system · Standards · Distributed · Security protection

14.1 Introduction

The evolution of the power delivery networks supposes the transition from the centralised control to the microgrids control. The introducing of the microgrids offers the flexibility, the autonomy of power supply, increased dynamical response due

M. Gaiceanu (✉) · I. N. Arama
Department of Automation and Electrical Engineering, Dunarea de Jos University of Galati, Galati, Romania
e-mail: marian.gaiceanu@ugal.ro

I. N. Arama
e-mail: iulian.arama@ugal.ro

I. Ghenea
Doctoral School of Fundamental and Engineering Sciences, Dunarea de Jos University of Galati, Galati, Romania
e-mail: gheneaiulian@yahoo.com

N. Mahdavi Tabatabaei et al. (eds.), *Microgrid Architectures, Control and Protection Methods*, Power Systems,
https://doi.org/10.1007/978-3-030-23723-3_14

to the power electronics interfaces. For the transmission and distribution systems, depending on the nature of the load, and to the choose energy way the types of the microgrids are as following: DC, AC and hybrid DC and AC-coupled.

The distributed energy system (DES) is the main component of the microgrid architecture. Besides DES, the microgrid contains the energy storage system (ESS), and loads (linear or/and nonlinear). Distributed energy systems are based on photovoltaic panels, wind turbines, hydro turbine, fuel cell, micro-CHP, biomass, Stirling engines so on. Thus, the microgrid architecture enables the integration of renewable sources, fossil fuels and biofuels. The storage system has the role of balancing (stability) power fluctuations from renewable energy sources. The storage system is sized so that it can feed most of its loads autonomously for a certain amount of time. The main storage systems are batteries, super capacitors, flywheels, compressed air, thermal, pumped hydro.

The structure of this chapter is as follows: overview Section, followed by the current state of microgrids control architectures Section; the hierarchical control is very specific to the microgrid; the specific standards are mentioned in the dedicated Section; as case study, the robust state-feedback (SF) control of the DC microgrid has been employed. For the modern microgrids, the Cyber-Physical System is presented. The chapter ends with the Reference Section.

14.2 Overview

The microgrids include the important environmental, technical and economic benefits through increased energy efficiency and reduced CO_2 emissions, being considered as safe power source.

The load into a microgrid is variable. Therefore, the microgrid will have to distribute energy in a balanced way (without overload), ensuring the stability and continuity of the energy supply (increasing the quality of services).

The main types of the DC microgrids control architectures are classified as follows: centralized, decentralized and distributed [1]. All DC Power Systems (PSs) are not facing problems such in AC PSs. Therefore, the reactive power control, frequency issues as stability and synchronization are disappeared in DC PSs [2]. Taken into consideration the above mentioned advantages, the DC PSs are very attractive. The PSs are vulnerable to natural disasters, being exposed to the blackouts. The microgrids are the solutions to reduce the risk of blackouts, are friendly environment, increase the energy efficiency, and integrate the renewable energy sources.

14.3 Architectures of the DC Microgrids

In an energy system, generator control and economic energy delivery can be achieved through a centralized method (Fig. 14.1) [3]. Through this method, in order to process the data, the central controller receives all the information from the entire system. The Supervisory, control and data acquisition system (SCADA) will send the control signals from each agent. This advanced automation control system manages the control, acquisition and monitoring of the operation of the power supply system [4]. Each agent will use a bidirectional communication channel to transfer data to the central computer system. This control architecture is disadvantageous for systems with high number of agents. The centralized structure is not reliable, economical, and inflexible. The simplicity of control and the economic delivery of energy are the main advantages. To make a decision on the entire centralized system, the system uses global information.

As mentioned above, the decentralized method is a control way of the microgrid. In this control type a particular agent or sub-system self-regulates, which means that in order to gain more market profit and more stability, the individual agent decides the actions based on data (voltage, frequency) taken locally [5].

The decentralized method has no communication links; it does not send information to agents. The method consists in controlling the sources from the data obtained on the basis of local measurements (voltage, frequency). However, it is based on some agents, called leader agents, who receive and send information. The method does not ensure global stability and optimization, but only local (even if the link with some leading agents is lost, stable microgrid remains). Advantages include the protection of agents' data, ensuring system stability. Instantaneous power can be balanced between sources connected in parallel in both DC and alternating currents (AC) with this control strategy. In DC power microgrids, the power balance of parallel connected, decentralized output sources is implemented using voltage drop control [6–8]. With regard to power management within microgrids with energy stor-

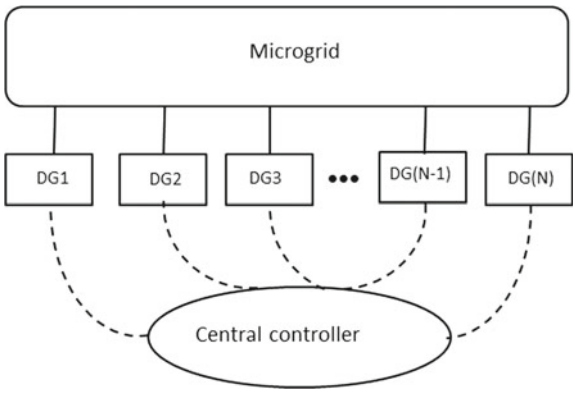

Fig. 14.1 Centralized control

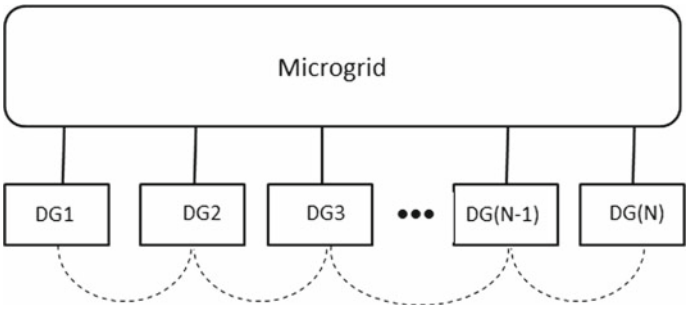

Fig. 14.2 Decentralized control

age elements, if the loads exceed the maximum system power, the storage system is discharged. The storage system is charged when there is extra energy from sources.

As agent a generator, a consumer, or a microgrid could be taken into account.

On the decentralized method (Fig. 14.2), to perform the objectives (increased market profit, system stability assurance) the individual agents decide the actions based on the locally data [3]. The centralized method collects the global information in order to control the entire system. The decentralized method does not require the data exchange (locally or globally) between the agents or with the central room control. There are only special agents (leaders) which may exchange the data through the center.

One disadvantage of the decentralized method is that the entire stability or optimization is not assured, but only locally. The reason is simple: no data communication exchanges exist. More deeply, each method has its own advantages and disadvantages the decentralized method has to be taken into account. From point of view of security data, the decentralized systems protect the confidentiality of the agents by acquiring privileged data [9–11]. In addition, the stability of the decentralized system (DS) is higher than the similar centralized system (CS); the reason is very simple, if there are leaders without connection with any agents, the distribution system is being capable to maintain the stability due to the local stability assures by the other agents. Figure 14.2 shows the decentralized method principle [3].

One other reason to implement distributed control is its expandability feature (plug-and-play feature). By using this concept into the conventional power system (PS), more flexibility is assured. Moreover, new alternative energy can be introduced in the PS or to the local consumers. One agent is considered one bidirectional energy port (i.e. the energy entrance from the generators or energy delivery to the users). In the distributed control method, also known as the consensus control, the necessary local information transmitted to the agents can be obtained from the local parameter measurement (e.g. voltage and frequency) or from the neighbours. In Fig. 14.3 one example of the distributed control system (DCS) using the local information through the communication links is shown [3, 9].

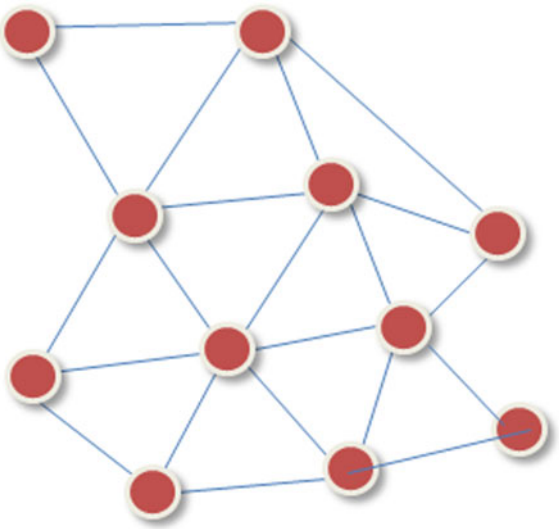

Fig. 14.3 Distributed control system

In the DCS, the information shared by the local agents to the others is bidirectional. In the decentralized systems there is no communication between the agents, each agent can use only the local measurements. In turn, in the distributed systems the users can share the information. In this manner, the global optimization methods could be applied in the distributed systems. This qualitative task is allowable also in the centralized method. The expandability of the distributed system architectures through plug and play feature will not influence the operation of the smart grid thanks to existing local information. Therefore, the smart grid could be extended easily through the new agents that can be connected to the grid. Figure 14.3 shows how a simple microgrid with the distributed method can be equipped [3, 9].

The advantage of using distributed control is to ensure the micro-relay function even when the node's controller no longer performs its functions. As a disadvantage, control is dependent on the distributed communications system.

14.4 Hierarchical Control

The coordinated control is classified according to the specified objectives: decentralized, centralized and distributed type. Taking into consideration the fluctuation and discontinues of the energy provided from renewable energy sources (RES) the energy storage system is necessary. The delivered electrical energy by the RES can be included in the utility network through the static power converters. In order to deliver the maximum extracted energy different maximum power point tracking (MPPT) methods are involved. From control point of view the main power sources

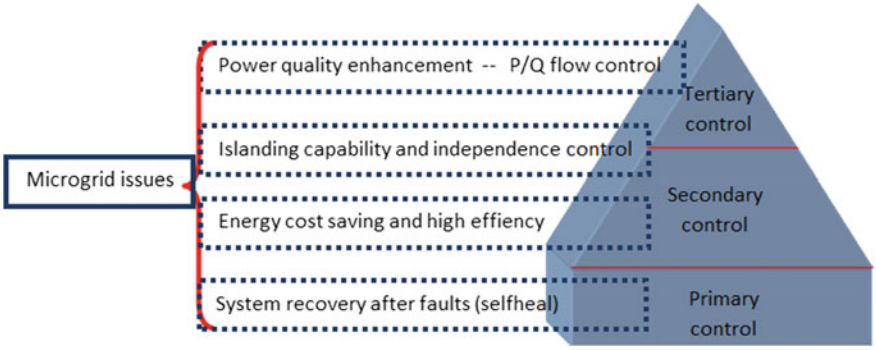

Fig. 14.4 The hierarchical control: main concerns

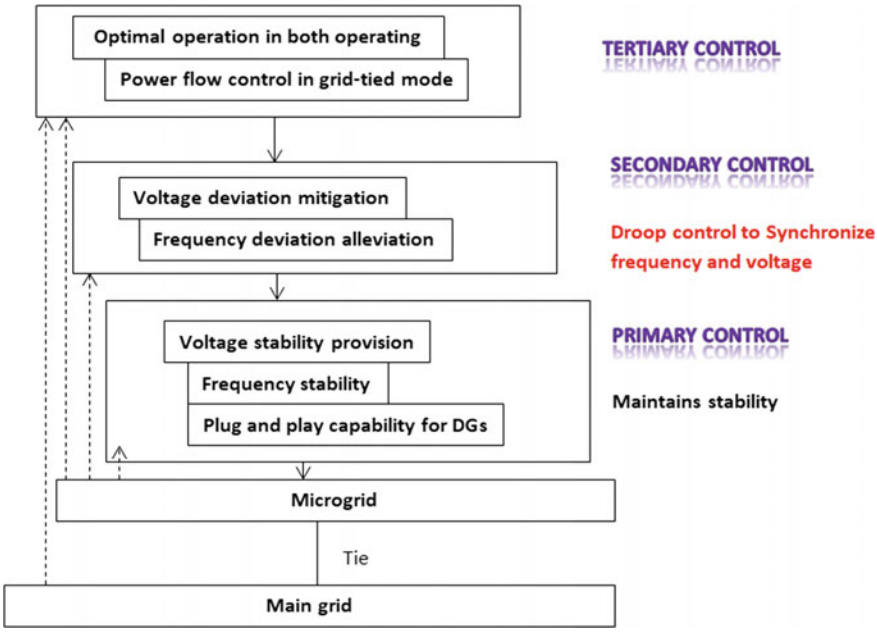

Fig. 14.5 The hierarchical control: main features

of the PS are controlled by the primary control. The photovoltaic panels, the batteries and the fuel cells provide DC power and can insert in the DC microgrid by using one or two-stage power conversion. Depending on the size of the microgrid, the small size microgrid are controlled by using master-slave control [4].

Hierarchical control is often used in DC power microgrids. This method uses 3 control types [12]: primary control, secondary control, and tertiary control (Fig. 14.4). Figure 14.4 contains the main concerns of the microgrids [13]. The Fig. 14.5 comprises the features of each level from the hierarchical control [13].

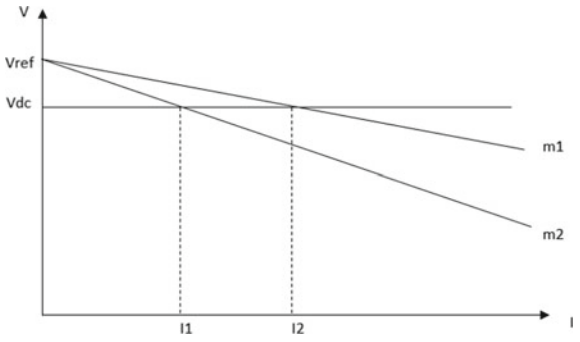

Fig. 14.6 The load distribution function on the droop constants

This hierarchical control (Fig. 14.5) can be implemented in both centralized architecture and distributed architecture. Centralized architecture faces uncertainty about the availability of renewable energy sources, load demands. This type of architecture has the deafness of a delayed response to problems [10]. The distributed control approach does not need a central controller and needs less information (communication) than in the centralized case. For stabilization purposes, the primary control (PC) as part of the hierarchical architecture is almost similar with the decentralized one. In the hierarchical control architecture, PC (for stabilization purposes) is almost similar with the decentralized control. As primary control, the voltage droop control (VDC) is used [8, 11]. By using the VDC, by using different droop constants (m_1 or m_2, Fig. 14.6) the load distribution can be performed.

In order to ensure both local operation and interconnection between distributed sources parallel connected, the proposed control block diagram [7, 14] has in view the balanced distribution of power or load between the connected parallel converters (Fig. 14.7) [7]. The control system contains local control loops and an external voltage loop (Fig. 14.7) [7]. However, this method cannot achieve a balanced distribution of loads, especially in systems with different values of line resistances. Many improvements have been made to this method [15], including an adaptive power balance control [15, 16].

In any case, almost the same with the AC power supply, the PC in the DC system cannot assure the zero steady state error. Therefore, the stationary regime the voltage error is obtained. In order to obtain the zero steady state voltage error, the secondary distributed control (voltage and frequency synchronization) is introduced. The most commonly used method is the consensus control [9, 10]. In this type of control there is a global control objective (e.g., the global voltage deviation), and one agent works with his local estimate. In the DC PS, one agent can be a distributed source, user or microgrid. Through this method, the control variable value will be the same for all agents thanks to available information from the neighbors [17, 18]. For this control type, the global voltage averages is necessary. This value can be estimated from the exchangeable information between the neighbors and from the local data. The necessary data between the microgrids is obtained through a dynamic consensus-based protocol [19]. By introducing Proportional Integral (PI) controller, the cancellation

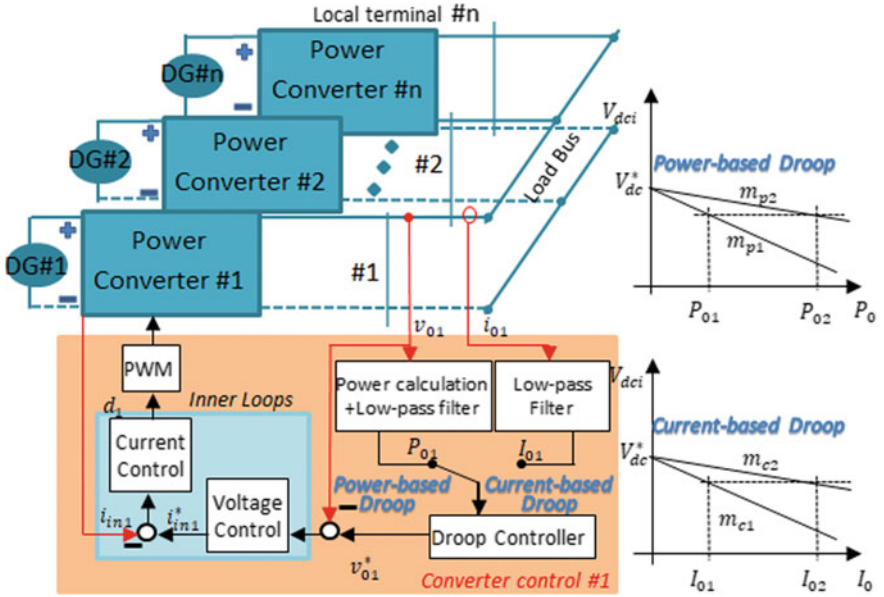

Fig. 14.7 The droop control method (power or current—based droop) applied in DC microgrid

of the voltage error (obtained by subtracting the estimated voltage from the reference value) takes place. In order to restore the average tension by respecting the load sharing, the discrete consensus method is used [20]. The optimal task is performed by the tertiary control. The tertiary control delivers a reference for the system by using power flow control (between the microgrids or between the distributed sources within a microgrid) [21–23].

14.5 Standards

Microgrids are island systems for local utility or energy distribution systems and contain at least one distributed power source and a corresponding load.

By performing the connection or disconnection of the power sources from a microgrid with minimum interruption from the PS, the reliability of the microgrid is increased [24, 25].

Network interconnection standards (IEEE 1547) are the optimum way for engineers, to perform fast the tasks of custom engineering, to prepare and obtain the specific approval processes, with minimal costs.

The planning and operation of the microgrids are included in IEEE 1547.4 standard. The IEEE 21 Standards Coordination Committee (SCC21) develops a guide

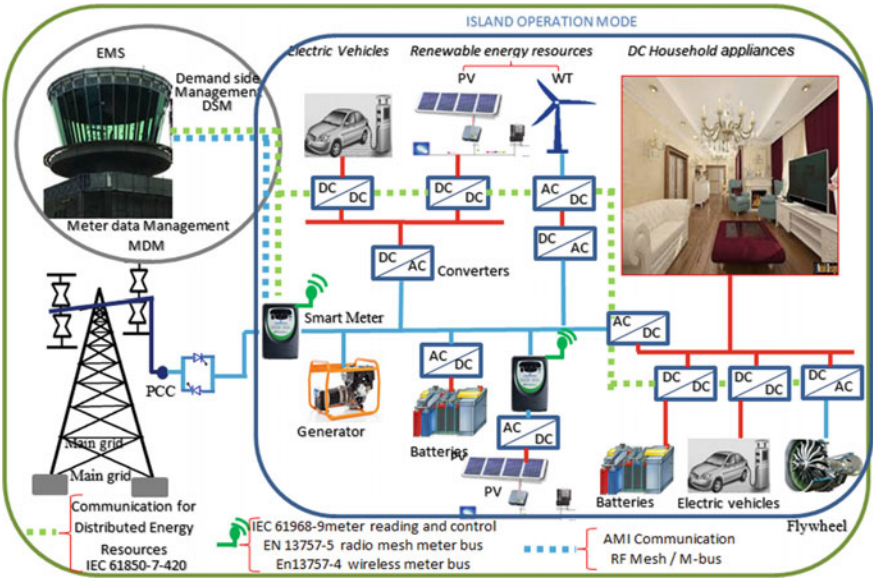

Fig. 14.8 Topology of the Intelligent microgrid

to help the operators of the PS, the specialists, and the manufacturers to use the technical aspects of the microgrid operation and implementation.

The communications standards at the microgrid level are mentioned and represented the associated flux in the Fig. 14.8:

- IEC 61850-7-420 Communications for Distributed energy Resources,
- IEC61968-9 m reading control,
- EN13757-5 radio mesh meter bus,
- EN13757-4 wireless meter bus.

14.6 Three-Phase Grid Active Power Converter: Case Study

In this Section the authors consider the DC microgrid, operating in both modes: grid-connected and standalone (island mode). The microgrid components are the Three-Phase Grid Active Power Converter (TP-GAPC), the back-up PS and the active load. The power flow continuity through the system is assured by introducing a back-up PS. The photovoltaic panels, and battery bank have been considered for back-up PS.

14.6.1 The TP-GAPC Mathematical Model Description

The modern vector control theory is employed. The synchronous reference frame and decoupled loop techniques are envisaged.

Firstly, the TP-GAPC mathematical description is based on the synchronous reference frame, the coupled dynamical Eq. (14.1) are as follows:

$$\begin{aligned} \frac{dI_d}{dt} &= -\omega \cdot I_q - \frac{1}{L} \cdot V_d + \frac{1}{L} \cdot E_d \\ \frac{dI_q}{dt} &= \omega \cdot I_d - \frac{1}{L} \cdot V_q + \frac{1}{L} \cdot E_q \end{aligned} \tag{14.1}$$

The above mentioned differential form can be expressed as state-space mathematical model:

$$\begin{aligned} \begin{bmatrix} \dot{I}_d \\ \dot{I}_q \end{bmatrix} &= \begin{bmatrix} 0 & -\omega \\ \omega & 0 \end{bmatrix} \cdot \begin{bmatrix} I_d \\ I_q \end{bmatrix} + \begin{bmatrix} -\frac{1}{L} & 0 \\ 0 & -\frac{1}{L} \end{bmatrix} \cdot \begin{bmatrix} V_d^* \\ V_q^* \end{bmatrix} + \begin{bmatrix} \frac{1}{L} & 0 \\ 0 & \frac{1}{L} \end{bmatrix} \cdot \begin{bmatrix} E_d \\ E_q \end{bmatrix} \\ y &= \begin{bmatrix} 1 & 0 \\ 0 & 1 \end{bmatrix} \cdot \begin{bmatrix} I_d \\ I_q \end{bmatrix} \end{aligned} \tag{14.2}$$

where, V is the converter voltage, E is the source voltage, I is the line current and ω is the grid pulsation.

The Eq. (14.2) contains both the state variable and the output of the grid active power converter (GAPC). Therefore, the standard state-space form representation of the dynamical system can be written as:

$$\begin{aligned} \dot{x}(t) &= A \cdot x(t) + B \cdot u(t) + F \cdot e(t) \\ y(t) &= C \cdot x(t) + D \cdot u(t) \end{aligned} \tag{14.3}$$

in which the components of the control vector are the dq converter voltages:

$$u = \begin{bmatrix} V_d^* \\ V_q^* \end{bmatrix} \tag{14.4}$$

the components of the disturbance vector are the dq grid voltages:

$$e = \begin{bmatrix} E_d \\ E_q \end{bmatrix} \tag{14.5}$$

and, obviously, the output vector, y, of dynamical system consists of the dq current components solution. The control vector does not affect the output; therefore, $D = 0$.

Based on the knowing dq current and voltage components, the AC grid power can be deducted:

$$P_{AC} = \frac{3V_d \cdot I_d + 3V_q \cdot I_q}{2} \tag{14.6}$$

The DC-link power is the product of the known DC-link voltage and of the output DC:

$$P_{DC} = V_{DC} \cdot I_{OUTDC} \tag{14.7}$$

By neglecting the power loss in the GAPC, the ac grid power (input) equals the DC link power (output). Therefore, by inserting the Eq. (14.7) into Eq. (14.6), the unknown variable (output DC current, I_{OUTC}) is obtained:

$$I_{OUTDC} = \frac{3}{2V_{DC}} \cdot \left(V_d \cdot I_d + V_q \cdot I_q\right) \tag{14.8}$$

In order to obtain a decoupled system, some additional terms are required (voltage decoupling terms). In this manner, the decoupled synchronous reference frame current loops are attained:

$$\begin{bmatrix} \dot{I}_q \\ \dot{I}_d \end{bmatrix} = \begin{bmatrix} \frac{1}{L} & 0 \\ 0 & \frac{1}{L} \end{bmatrix} \cdot \begin{bmatrix} E_q \\ E_d \end{bmatrix} - \begin{bmatrix} \frac{1}{L} & 0 \\ 0 & \frac{1}{L} \end{bmatrix} \cdot \begin{bmatrix} V_q \\ V_d \end{bmatrix} \tag{14.9}$$

By analyzing the DC-link circuit node, the relation between the currents can be obtained:

$$C \cdot \frac{dV_{dc}}{dt} = I_{INDC} - I_{OUTDC} \tag{14.10}$$

The voltage across the DC-link capacitor (14.7) is obtained from the applied power balance [11]:

$$\frac{dV_{dc}}{dt} = \frac{1}{C} I_{RES} - \frac{3V_d \cdot I_d + 3V_q \cdot I_q}{2C \cdot V_{dc}} \tag{14.11}$$

in which I_{RES} [A] is the instantaneous current from Renewable Energy Source (RES).

The utility voltage components are calculated taking into consideration the fulfilled mission of the PLL (phase-locked loop) [11]:

$$E_q = E, \quad E_d = 0, \tag{14.12}$$

active component of the source voltage vector has the RMS value (E) of the source voltage.

14.6.2 Robust Control of the Active Three-Phase Power Converter Supplying the Active Load

The authors proposed a robust solution to disturbances effect. It derives from the conventional linear control of the three-phase power converter [26–28] connected to the grid. Based on the input error, an integral term has been added.

$$\dot{\mathbf{z}}(t) = y^*(t) - y(t) \tag{14.13}$$

By considering the output equation of the GAPS (14.2), one more state vector has been added to the dynamical system:

$$\dot{z}(t) = y^* - C \cdot x(t) \tag{14.14}$$

Therefore, the new dynamical model in standard state space is obtained:

$$\begin{cases} \begin{bmatrix} \dot{x}(t) \\ \dot{z}(t) \end{bmatrix} = \begin{bmatrix} A & 0 \\ -C & 0 \end{bmatrix} \cdot \begin{bmatrix} x(t) \\ z(t) \end{bmatrix} + \begin{bmatrix} B \\ 0 \end{bmatrix} \cdot u(t) + \begin{bmatrix} F \\ 0 \end{bmatrix} \cdot e(t) + \begin{bmatrix} 0 \\ I \end{bmatrix} \cdot y*(t) \\ y(t) = \begin{bmatrix} C & 0 \end{bmatrix} \cdot \begin{bmatrix} x(t) \\ z(t) \end{bmatrix} \end{cases} \tag{14.15}$$

In this condition, the new state feedback control, namely integral state space control, is derived:

$$u(t) = \sum_{i=1}^{3} u_i(t) \tag{14.16}$$

The new control contains three components, each of them having a certain role. The classical state feedback control is nominated by u_1, being placed on the state feedback:

$$u_1(t) = G \cdot x(t) \tag{14.17}$$

The task of the u_2 control component has in view the reference tracking and it is inserted on the reference,

$$u_2(t) = K \cdot y^*(t) \tag{14.18}$$

The last control component, u_3, is placed on the disturbance vector, in order to compensate it [26–28]

$$u_3(t) = R \cdot e(t) \tag{14.19}$$

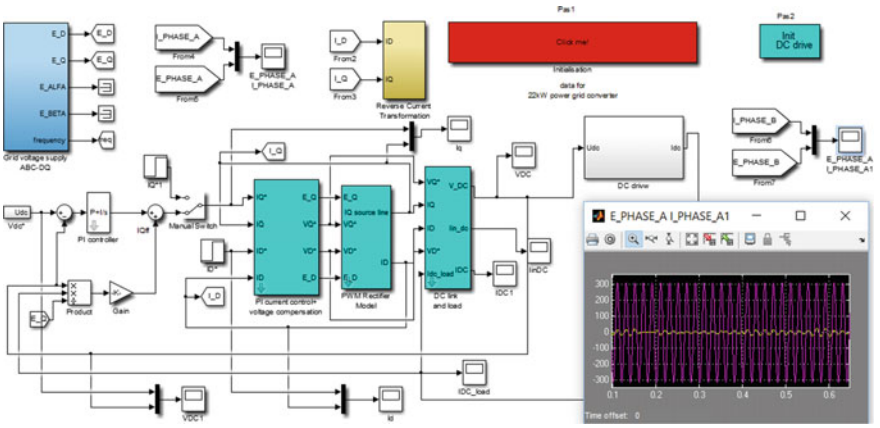

Fig. 14.9 The microgrid Simulink implementation: AC–DC power converter, PV back-up PS supplying the active load

By using an appropriate design, the matrix gain R can be deducted. The main role of it is to compensate the perturbation effect [27] (Fig. 14.9).

$$R = -B^{-1} \cdot F \tag{14.20}$$

By introducing the Eqs. (14.17)–(14.19) into Eq. (14.16), the grid power converter control is obtained [28, 29]:

$$u(t) = Gx(t) + Kz(t) + Re(t) = \tilde{G}\tilde{x}(t) + Re(t) \tag{14.21}$$

where, the matrices G, K, R are obtained as in [26–29], the augmented state $\tilde{x}(t) = \begin{bmatrix} x(t) \\ z(t) \end{bmatrix}$, and the obtained robust control matrix $\tilde{G} = \begin{bmatrix} G & K \end{bmatrix}$.

This type of control is known as integral SF. Figure 14.10 depicts very clear the action of the integral SF control on the dynamical system [26–29].

14.6.3 Design of the Gain Matrices

The first control component, the SF, assures the stability and dynamic performances of the utility converter. The SF control is based on the desired pole placement. Based on the imposed performances (time response T_R, and damping factor d) the desired poles are deducted:

$$\lambda_{1,2} = -d \cdot \omega_0 \pm \omega_0 \cdot \sqrt{1 - d^2} \tag{14.22}$$

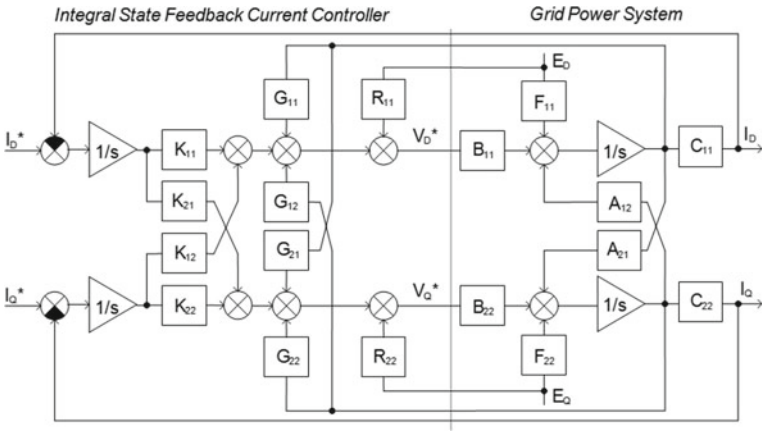

Fig. 14.10 Robust SF current loop control of the utility grid converter

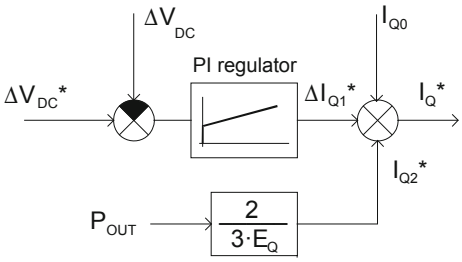

Fig. 14.11 The PI voltage controller with the power feedforward component

with

$$\omega_0 = \frac{1}{d \cdot T_R} \cdot \left[3 - \frac{1}{2} \ln\left(1 - d^2\right) \right] \tag{14.23}$$

The second control component has in view the cancelation of the steady-state error (i.e. the output of the current loop will be equal with the imposed reference). This task is performing by adequate design of the K gain matrix:

$$K = -B^{-1} \cdot (A + B \cdot G) \cdot C^{-1} \tag{14.24}$$

The third control component has in view the disturbance rejection and uses the Eqs. (14.19) and (14.20).

Additionally, one load current component is inserted in order to obtain a fast dynamic response to load variations. This component, feedforward, is obtained from power balance concept and it is added to the reference (Fig. 14.11). In this manner, all the time, power of the utility converter meets the requirements of the power load. The feedforward current component is:

$$I_{q2}^{*} = \frac{2}{3E} \cdot P_{out} \tag{14.25}$$

The Eq. (14.25) shows that the feedforward current component controls indirectly the active power. At the same time, the output power, P_{out} (see the Fig. 14.11), can be calculated, measured or estimated.

By imposing a zero *d*-axis current reference value the power quality requirement is fulfilled by the utility converter:

$$I_{d}^{*} = 0 \tag{14.26}$$

The Eq. (14.26) will conduct to unity power factor operation.

14.6.4 The Voltage Control

The main task of the DC link voltage loop is to control the DC link voltage. The second task is to eliminate the disturbances. Therefore, technical specifications should contain the imposed undervoltage and overvoltage limits during the load transitory regimes.

14.6.5 The Proportional-Integral (PI) Voltage Controller with Power Feedforward

The added component into the voltage loop, the load power feedforward component, P_{out}, has in view the fast compensation of the load variations. Therefore, the fast time response is obtained to load variations. The PI voltage controller with power feedforward is represented in Fig. 14.11 [26, 27].

The output feedforward signal results as follow:

$$I_{Q2}^{*} = \frac{2}{3 \cdot E_{Q}} \cdot P_{OUT} \tag{14.27}$$

$$P_{OUT} = I_{outdc} \cdot V_{dc} \tag{14.28}$$

The expression of the PI controller is as follows:

$$\frac{\Delta I_{Q}^{*}}{\Delta e_{V_{dc}}} = C_{PIv}(s) = K_{pv}(1 + \frac{1}{T_{iv}s}) \tag{14.29}$$

where, $e_{V_{dc}}$ is voltage error V_{dc}, that is $e_{V_{dc}} = V_{dc}^{*} - V_{dc}$. Therefore, the outline to blocks of the controlled complete system is that one shown in Fig. 14.12 [26, 27].

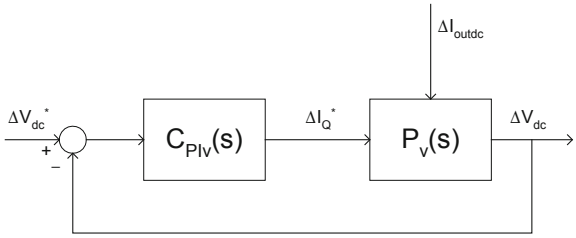

Fig. 14.12 Outline to the controlled system blocks (voltage and current loops)

The DC link voltage controller is based on PI control. In order to find the controller parameters (proportional gain K_{pv}, and integral time, T_{iv}), the adequate performances should be imposed:

1. The phase magnitude φ_{mv} (in radian)
2. The bandwidth ω_{cv} (in radian per second).

Based on the Refs. [26–29], the controller parameters K_{pv}, and integral time, T_{iv} are obtained:

$$T_{iv} = \frac{1}{\omega_{cv} \cdot \tan(\varphi_c - \varphi_{mv})} \tag{14.30}$$

$$K_{pv} = \frac{T_{iv} \cdot \omega_{cv}}{M \cdot \sqrt{1 + (T_{iv} \cdot \omega_{cv})^2}} \tag{14.31}$$

where M and φ_c are the module and phase (in radian) of the PS, $P_v(s)$, under control.

The DC-link voltage loop is a nonlinear system. Therefore, the linearization method (small perturbation method around equilibrium point) should be applied.

The basic initial values are the imposed response time $T_r = 0.55\text{e}{-3}$, and the desired damping coefficient $d = \sqrt{2}/2$. Based on the desired performances, the imposed closed loop poles are deducted $P = [\text{l1 l2 l3 l4}]$. The input inductance is a key design factor. Based on its value, the integral SF controller has been designed. Thus, the necessary matrices (G, K, and R) are obtained.

14.7 Simulation Results

The proposed control of the three-phase utility power converter has been developed and tested in Matlab program environment (Fig. 14.9). The 22 kVA apparent power (S_n) of the TP-GAPC has been taken into account. The $C = 1565$ μF, DC-link capacitor value is considered. The parameters of the real line inductance are $R_{in} = 0.001$ Ω, $L_{in} = 2.1$ mH. The load is driven by a $P_n = 1$ [kW] DC machine, rated power. The TP-GAPC has a battery bank PS as backup power. Considering around 300 min load autonomy in case of grid failure, 4 series batteries have been chosen (MK 8A27DT-DEKA 12 V 92Ah AGM). By taken into account a grid failure

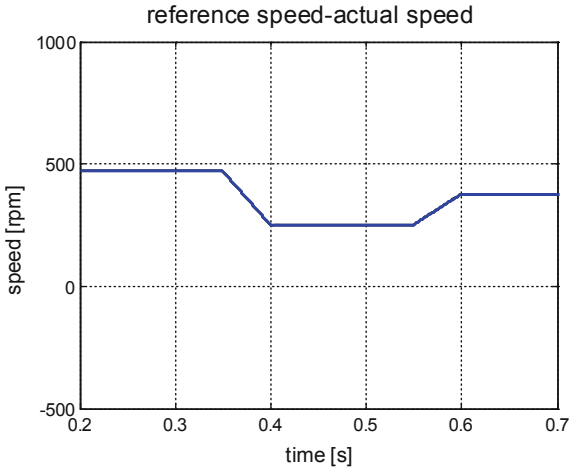

Fig. 14.13 Comparison between speed reference and the feedback speed

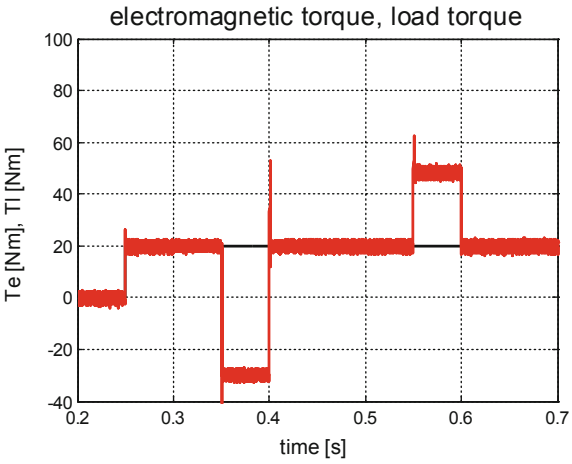

Fig. 14.14 Electromagnetic torque and load torque comparison

the entire microgrid PS has been numerical simulated (based on Matlab-Simulink software) [29]. In Figs. 14.13, 14.14, 14.15, 14.16, 14.17 and 14.18 the obtained simulation results are presented.

Taken into account the speed reference of the DC machine, the speed control loop assures the fast reference tracking in both dynamic and steady-state regimes (Fig. 14.13). The numerical validation of the mechanical motion equation is shown in the Fig. 14.14. During the steady state regime, the load torque is the same as the electromagnetic torque. The unity power factor operation of the utility converter is demonstrated in Fig. 14.15. The performances of the DC link voltage controller are shown in the Fig. 14.16. In Fig. 14.17 the bidirectional energy transfer is demonstrated. The performances of the active current controller for the utility grid are shown in Fig. 14.18. Voltage outage has been simulated at the moment

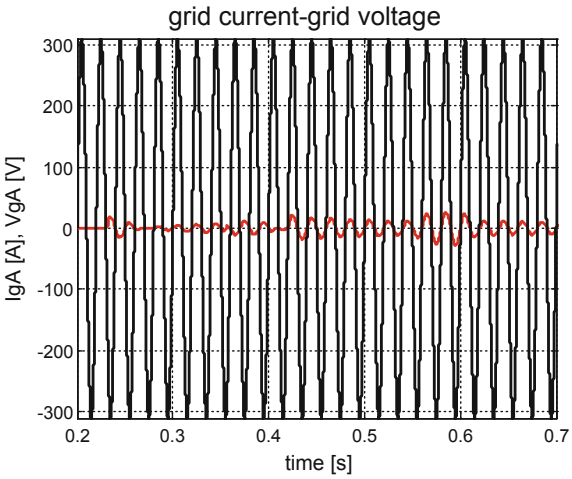

Fig. 14.15 Unity power factor in any operating conditions

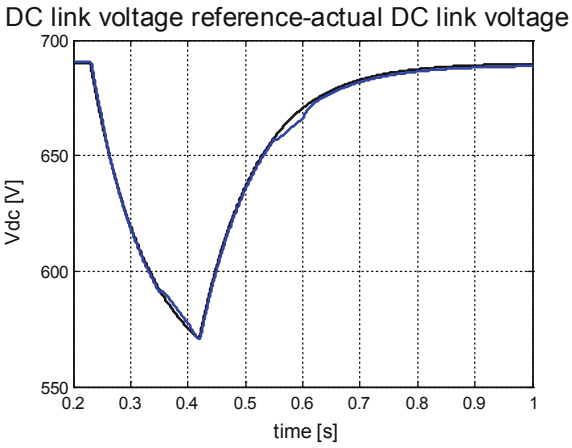

Fig. 14.16 DC link voltage, VDC [V]

$t = 0.22$ s (Fig. 14.16). The obtained numerical results prove the well design of the back-up system.

14.8 Cyber-Physical System

The future requirements for the smart grid design are well identified by Department of Energy (DOE) of the US [30, 31]. Nowadays, the most important future is the resistance to attack. One functional requirement is to restore the normal operation through self-healing feature. The other features are as in PS: power quality assurance

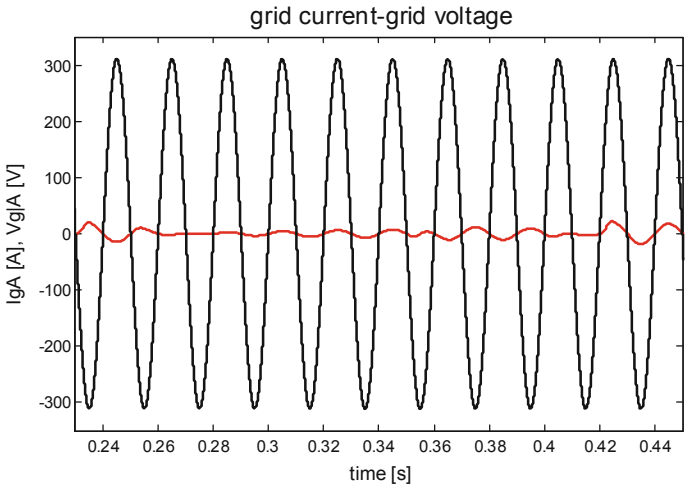

Fig. 14.17 The unity power factor (magnified area): bidirectional power flow

Fig. 14.18 Active current controller: the reference and the feedback

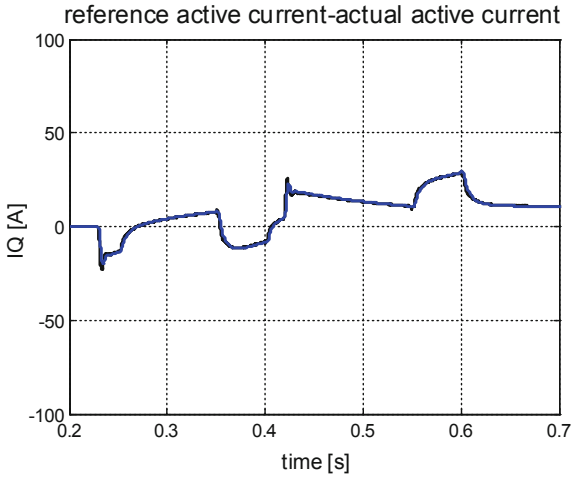

of PS, win-to-win strategy related to consumers, generation resources and backup capability through the storage system, access to energy markets in an optimal way.

In order to satisfy the above mentioned requirements advanced metering infrastructures (AMIs), Phase Measurement Units (PMUs), wide-area measurement systems (WAMS) are used. At the same time, the introduction of AMIs will get the PS more vulnerable to attack [32]. The PMUs are used both for real time measurements in order to estimate the state of the PS, and for increasing of the PS safety by avoiding cyber-attacks. The WMS will allow collecting the parameters of the transmission line in dynamic regimes.

A holistic approach within an energy grid, regarding the security of it, needs to study cyber-physical system (CPS) interactions to properly quantify the impact of attacks [33] and evaluate the effectiveness of countermeasures.

An analysis of system vulnerability should begin by identifying cyber resources (software protocols, hardware and communications protocols). Potential environmental security issues can be investigated by testing penetration and vulnerability scanning. In order to identify the additional vulnerabilities of the PS, a rigorous and continuously analysis of the information about the security of the providers, the system logs and the implemented intrusion detection systems are necessary.

A PS consists of three parts: generation, transmission and distribution.

The power supply system contains several control loops connected to different communication signals and protocols. It can be said that cyber-attacks directed to these control loops have a major influence on the stability of the electrical system throughout the system.

The data received by the central controllers comes from the installed sensors into PS. By using the adequate algorithms, the central controllers delivers the appropriate decisions to the field equipment. In Fig. 14.19, one representative control loop which includes both the physical system and the central controller (CC) is shown [34]. In Fig. 14.19, there are the sizes of command and exit of the physical system (substations, transmission lines and other physical machines). With the data acquisition system, system voltage and power are transmitted to the central control system via dedicated communication protocols.

In the CC, based on the measurements made, the data are processed by means of numerical algorithms. In this way, adequate control is given to the physical elements of the system. These algorithms are integrated into the Energy Management System (EMS). An opponent could exploit vulnerabilities along communications links by creating attacks (integrity attacks to compromise the content or denial or delayed communication with the equipment field, like denial of service—DoS). The DoS attack will compromise the synchronization between the measurement and control signals [35].

The impact of the attacks on the PS should be analysed for further security strategy approach. The results of the analyses conduct to the adequate defend countermeasures

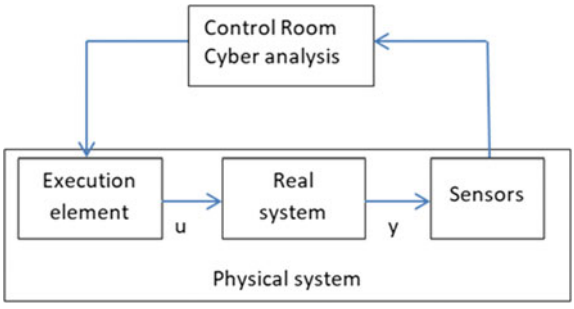

Fig. 14.19 The cyber-physical system

of the PS. The improper data detection methods can be used as a countermeasure. Therefore, for control purposes the new attack-resistant algorithms will be used.

The energy distribution system provides energy to the customer. In an intelligent network, there are common con loops of the end-user task.

To ensure the security of the network, at the level of communication protocols and parameters, some specific keywords are included.

(1) *Load shedding*. This expression is used in the distribution system in order to avoid the collapse of the energy system. To do this, emergency load charging circuits are used. These circuits are classified proactively, reactively, and manually. The proactive emergency line uses the automatic relay to maintain the normal operation of the distributed system. If the generation power sources are less than the connected load, an adequate frequency relay will disconnect the user distribution feeder in order to restore the normal frequency value. CPS use modern networks (they work on well-established Internet communications protocols (IP) such as IEC 61850).
In Fig. 14.19 present the interaction between Cybernetics and the Physical Part in a Cyber-Physical System [33].

(2) *Advanced metering infrastructures* and *demand management*: The use of AMIs assures the increased security of the distributed energy systems, penetration of the RES, and real time data consumption monitoring (by using smart meters—SMs—placed at the user locations). SMs are capable to switch off the users when there is no-load. Cyber-metering infrastructure is linked to consumer energy through a cyber-physical connection according to demand management [32]. The meter data management system (MDMS) controls the configuration of the meters. MDMS is network controlled. MDMS distributes the operational commands to SMs and processes the received data from the meters placed into the infrastructure. The technologies used by AMI can be: WiMax, mesh RF network, WiFi and power line. In order to transmit both power usage operations and meter-to-MDMS operation application layer protocols will be used (C12.22 or IEC 61850).

An intelligent smart grid requires a concept of layer protection, which consists of a cyber-infrastructure that limits opponent's access and increases resilience to power applications that are capable of functioning properly during an attack.

Sandia National Laboratories (SNL) owns the proprietary Energy Surety Microgrid technology™ (ESM) for managing a microgrid (connected to a grid or island operating modes) [35]. This technology uses a load connectivity hierarchy as well as a backup generation system. Developed microgrids through ESM methodology have high efficiency, increased reliability and strong cyber security.

A secure microgrid must be: simple, segmented, monitor operation, independent and reconfigurable.

14.9 Conclusions

The DC microgrid main architectures have been discussed. The specific control applied in DC microgrids has been presented. The requirements of the DC microgrids are presented in the Standards Section. One case study has been approached by the authors. It consists by robust SF control of the utility converter. The simulated power back-up system takes into account an active load [29]. During considered power supply outage the proposed microgrid maintain the performances in both sides: input and output of the PS. At the input, the necessary ac voltages are assured through the back-up PS (PV panels and battery power bank interfaced by the adequate power converters), by maintaining the adequate voltage amplitude and appropriate frequency. Moreover, the power quality constraints are maintained, the microgrid delivering the ac power at unity power factor.

Therefore, by introducing autonomous DC power sources (PV panels, and battery bank) an adequate autonomy of the active load has been assured. The above mentioned theory has been implemented in the Matlab-Simulink programming environment. The security of the microgrid is the most important task. A CPS has been presented related to the power system.

Acknowledgements This work was supported by a grant of the Romanian National Authority for Scientific Research, CNDI–UEFISCDI, project number PN-II-PT-PCCA-2011-3.2-1680.

References

1. A. Werth, A. Andre, D. Kawamoto, T. Morita, S. Tajima, M. Tokoro, D. Yanagidaira, K. Tanaka, Peer-to-peer control system for DC microgrids. IEEE Trans. Smart Grid **9**(4), 3667–3675 (2018)
2. Z. Wang, F. Liu, Y. Chen, S. Low, S. Mei, Breaking diversity restriction: distributed optimal control of stand-alone DC microgrids (2017), https://arxiv.org/abs/1706.02695. Accessed 2018
3. D. Wu, F. Tang, J.C. Vasquez, J.M. Guerrero, Control and analysis of droop and reverse droop controllers for distributed generations, in *IEEE 11th International Multiconference on Systems, Signals & Devices, SDD* (2014)
4. F. Valenciaga, P.F. Puleston, Supervisor control for a stand-alone hybrid generation system using wind and photovoltaic energy. IEEE Trans. Energy Convers. **20**(2), 398–405 (2005)
5. H. Pourbabak, T. Chen, B. Zhang, W. Su, Control and energy management system in microgrids. Institution of Engineering and Technology (IET) (2017), http://digital-library.theiet.org/content/books/10.1049/pbpo090e_ch3. Accessed 2018
6. R. Hidalgo Leon, C. Sanchez Zurita, P. Jacome Ruiz, J. Wu, Y. Munoz Jadan, Roles, challenges, and approaches of droop control methods for microgrids, in *IEEE PES Innovative Smart Grid Technologies Conference—Latin America (ISGT Latin America)*, Quito, Ecuador (2017)
7. T. Dragicevic, X. Lu, J.C.V. Quintero, J.M. Guerrero, DC microgrids—Part I: A review of control strategies and stabilization techniques. IEEE Trans. Power Electron. **31**(7), 4876–4891 (2016)
8. Q. Shafiee, T. Dragicevic, F. Andrade, J.C. Vasquez, J.M. Guerrero, Distributed consensus-based control of multiple DC-microgrids clusters, in *Annual Conference of the IEEE Industrial Electronics Society* (2014), pp. 2056–2062

9. L. Meng, T. Dragicevic, J.M. Guerrero, J.C. Vasquez, Dynamic consensus algorithm based distributed global efficiency optimization of a droop controlled DC microgrid, in *IEEE International Energy Conference* (2014)
10. X. Lu, K. Sun, J.M. Guerrero, J.C. Vasquez, L. Huang, Double-quadrant state-of-charge-based droop control method for distributed energy storage systems in autonomous DC microgrids. IEEE Trans. Smart Grid **6**(1), 147–157 (2015)
11. https://blog.482.solutions/distributed-ledger-technology-and-its-types-ad76565ae76. Accessed 2018
12. T.L. Vandoorn, J.C. Vasquez, D.M. de Kooning, J.M. Guerrero, L. Vandevelde, Microgrids: hierarchical control and an overview of the control and reserve management strategies. IEEE Ind. Electron. Mag. **7**(4), 42–55 (2013)
13. Z. Wang, F. Liu, Y. Chen, S.H. Low, S. Mei, Unified distributed control of standalone DC microgrids. IEEE Trans Smart Grid (2017)
14. J.M. Guerrero, J.C. Vasquez, J. Matas, L.G. de Vicuna, M. Castilla, Hierarchical control of droop-controlled AC and DC microgrids—a general approach toward standardization. IEEE Trans. Ind. Electron. **58**(1), 158–172 (2011)
15. Q.C. Zhong, Robust droop controller for accurate proportional load sharing among inverters operated in parallel. IEEE Trans. Ind. Electron. **60**(4), 1281–1290 (2013)
16. H. Kakigano, Y. Miura, T. Ise, Distribution voltage control for DC microgrids using fuzzy control and gain-scheduling technique. IEEE Trans. Power Electron. **28**(5), 246–2258 (2013)
17. R.S. Balog, P.T. Krein, Bus selection in multibus DC microgrids. IEEE Trans. Power Electron. **26**(3), 860–867 (2011)
18. M. Majid Gulzar, S. Tahir Hussain Rizvi, M. Yaqoob Javed, U. Munir, H. Asif, Multi-agent cooperative control consensus: a comparative review. Electronics **7**(22) (2018)
19. K. de Brabandere, B. Bolsens, J. den Keybus, A. Woyte, J. Driesen, R. Belmans, A voltage and frequency droop control method for parallel inverters. IEEE Trans. Power Electron. **22**(4), 1107–1115 (2007)
20. Z. Yan, D. Wu, Y. Liu, Consensus of discrete multiagent system with various time delays and environmental disturbances. Entropy **16**, 6524–6538 (2014)
21. S.G. Anand, B. Fernandes, J.M. Guerrero, Distributed control to ensure proportional load sharing and improve voltage regulation in low-voltage DC microgrids. IEEE Trans. Power Electron. **28**(4), 1900–1913 (2013)
22. S. Moayedi, A. Davoudi, Distributed tertiary control of DC microgrid clusters. IEEE Trans. Power Electron. **31**(2), 1–10 (2015)
23. G. Chen, E. Feng, Distributed secondary control and optimal power sharing in microgrids. IEEE/CAA J. Autom Sin **2**(3) (2015)
24. B. Kroposki, T.S. Basso, R. Deblasio, Microgrid standards and technologies, in *IEEE Power and Energy Society General Meeting—Conversion and Delivery of Electrical Energy in the 21st Century* (2008)
25. P2030 TM Smart Grid Interoperability Series of Standards. https://www.nrel.gov/docs/fy12osti/53028.pdf
26. M. Gaiceanu, Integral state feedback control of grid power inverter. Buletinul AGIR (3/2012)
27. F. Profumo, R.Uhrin, Complete state feedback control of quasi direct AC/AC converter, in *IEEE Industry Applications Conference, Thirty-First IAS Annual Meeting (IAS-96)* (1996)
28. M. Gaiceanu, Advanced State Feedback Control of Grid- Power Inverter. Energy Procedia **14**, 1464–1470 (2012)
29. M. Gaiceanu, C. Nichita, S. Statescu, Photovoltaic power conversion system as a reserve power source to a modern elevator, in *3rd International Congress on Energy Efficiency and Energy Related Materials (ENEFM2015)*. Springer Proceedings in Energy, Springer
30. S. Sridhar et al., Security of cyber-physical systems for the power grid. IEEE Process. **100**(1) (2012)
31. A modern network view system. National Energy Technology Laboratory (NETL), US Department of Energy (DOE) (2007)

32. NISTIR 7628, Guidelines for Intelligent Network Security. National Institute for Standards and Technology, August (2010)
33. GAO-11-117, Upgrading the Electricity Network: Progress has been made on the IT security guidelines, but key challenges remain to be addressed. US Government Accountability Office (GAO), January (2011)
34. D. Callaway, I. Hiskens, B who performs controllability of electrical loads. Proc. IEEE **99**(1), 184–199 (2011)
35. https://energy.sandia.gov/energy/ssrei/gridmod/integrated-research-and-development/esdm/. Accessed 2018